nature communications

Article

https://doi.org/10.1038/s41467-025-59577-6

Space weathering on the lunar nearside and farside constrained from Si isotopes

Received: 23 January 2025

Accepted: 29 April 2025

Published online: 07 May 2025

Check for updates

Hui-Yan Zhang[1], Hui-Min Yu[1,2] ✉, Hao-Lan Tang[1,2,3], Yu-Chao Lin[1], Zicong Xiao[1], Lin Yang[1], Jin-Ting Kang[1,2], Ji Shen[1,2], Liping Qin[1,2,3] ✉ & Fang Huang[1,2,3] ✉

Over long timescales, space weathering processes can modify the compositions of surface materials on the Moon. To assess the effects of space weathering of lunar soils, we study Si isotopes of Chang'E-5 (CE-5) and Chang'E-6 (CE-6) returned samples, and lunar meteorites. Here we show that both bulk soils from CE-5 and CE-6 exhibit heavier Si isotopic compositions than the basalt clasts within the soils and lunar meteorites, indicating that the space weathering obviously increase δ^{30}Si of lunar soils. Furthermore, the CE-6 soil from the lunar farside has heavier Si isotopic values than the average of CE-5 soils from the nearside, suggesting that the CE-6 soil has experienced a higher space weathering degree than the CE-5 soils. This increased weathering degree could be attributed to either a longer weathering period or stronger micrometeorite impacts on CE-6 soil from farside compared to CE-5 soils from nearside.

Space weathering, including micrometeorite impacts and solar wind irradiation, plays a critical role in planetary evolution. It shapes planetary surfaces, alters the compositions of surface materials, and contributes to the formation of surrounding atmospheres. Lunar regolith, commonly referred to as lunar soil[1], serves as a key resource for studying the interactions between space and the Moon during space weathering. Lunar soil, a fine-grained product formed from weathered local rocks mixed with exotic materials, preserves valuable information about surface processes. While space weathering does not significantly change the elemental concentrations of lunar surface materials, it has a pronounced effect on the isotopic composition of lunar soils (e.g., see refs. 2,3). Observations suggest that space weathering influences the isotopic compositions of several volatile elements, such as Fe, Mg, Cu, Zn, Cd, K, and Rb, leading to an enrichment of heavier isotopes in the residual of lunar soil (e.g., see refs. 2–7). Consequently, stable isotopes are a valuable tool for investigating the space weathering process.

Silicon isotopes are a sensitive tool to study the space weathering process, especially the possible different effects for lunar nearside and farside. During space weathering, Si can be lost through SiO vapor, which can produce significant isotopic fractionation[8,9]. The Chang'E-5 (CE-5) samples represent the youngest known mare basalts and have experienced less exposure time (see refs. 10,11) than Apollo samples. Understanding how this exposure time affects the composition of lunar surface materials is crucial. On the other hand, the CE-6 sample, the first ever returned from the Moon's farside[12], provides an important opportunity to evaluate space weathering processes on the lunar farside.

In this study, we analyzed Si isotopes in the CE-5 and CE-6 lunar soils to evaluate the space weathering effects on the lunar nearside and farside. For direct comparison, we also examined Si isotopes in rock clasts from CE-5 and CE-6 soils, as well as in six lunar meteorites. Our results reveal that space weathering produced a heavier Si isotopic signature in both CE-5 and CE-6 soils compared to rock clasts and lunar meteorites. The CE-6 soil exhibited a more pronounced isotopic shift than CE-5 soils, indicating a higher degree of space weathering. These findings demonstrate that Si isotopes serve as a novel tracer for deciphering space weathering effects on the lunar surface.

[1]State Key Laboratory of Lithospheric and Environmental Coevolution, School of Earth and Space Sciences, University of Science and Technology of China, Hefei, Anhui, China. [2]CAS Center for Excellence in Comparative Planetology, University of Science and Technology of China, Hefei, Anhui, China. [3]Institute of Deep Space Sciences, Deep Space Exploration Laboratory, Hefei, China. ✉e-mail: huy16@ustc.edu.cn; lpqin@ustc.edu.cn; fhuang@ustc.edu.cn

Results and discussion

Silicon isotope data of four bulk lunar soil samples (CE5C0100-YJFM00103, CE5C0400-YJFM00405, CE5C0400-YJFM00406, and CE5C0600) and one basalt clast (CE5C0800YJYX038) from CE-5, one bulk lunar soil (CE6C0400YJFM004) and rock clasts (CE6C0400YJFM004) from CE-6, and six lunar meteorites are listed in Table 1 and Fig. 1. Due to the small sizes of four clasts from CE-6, they were treated as one sample and digested together for Si isotope analysis. Figure 1 shows the Si isotopic compositions of the CE-5, CE-6 samples, and lunar meteorites, alongside Apollo samples[13–16]. All four CE-5 lunar soils and one CE-6 bulk soil exhibit higher δ30Si values than the CE-5 basalt clast, CE-6 clasts, and lunar meteorites. Among these, the CE-6 bulk soil has the highest δ^{30}Si value, surpassing both the Chang'E and Apollo samples (Supplementary Table 1 and Fig. 1). Although the δ^{30}Si value of CE-6 soil overlaps with some values of the CE-5 soils within errors, it is still higher than the average of CE-5 soils (Fig. 1). The δ^{30}Si of the CE-5 basalt clast is −0.33 ± 0.05‰ (2 SD), and the δ^{30}Si of the CE-6 clasts is −0.17 ± 0.01‰ (2 SD) (Table 1). The δ^{30}Si of lunar meteorites range from −0.29‰ to −0.19‰, consistent with the average δ^{30}Si of the bulk silicate Moon (BSMo), estimated at −0.28 ± 0.09 (2 SD) from Apollo samples[13–17], and the bulk silicate Earth (BSE), with a δ^{30}Si value of −0.29 ± 0.08‰ (2 SD)[18]. Among the six lunar meteorites, DAG400, NWA12971 and NWA13582 have slightly higher δ^{30}Si than the other three meteorites and BSE, but within the range of ferroan-anorthosites from Apollo samples (Fig. 1). The average concentrations of Al_2O_3, CaO and SiO_2 of the mixed CE-6 clasts are 16.6 wt%, 10.3 wt% and 53.1 wt%, respectively.

Table 1 | Silicon isotopic compositions of four CE-5 lunar bulk soil samples, one CE-5 lunar basalt clast sample, one CE-6 lunar bulk soil sample, one CE-6 clast sample, and six lunar meteorites in this study

Sample	Type	δ^{30}Si	2SD	δ^{29}Si	2SD	n
CE5C0100-YJFM00103	Lunar soil of CE-5	−0.05	0.05	−0.02	0.05	3
		−0.05	0.06	0.00	0.04	3
		−0.04	0.05	0.00	0.02	3
Average		−0.05	0.05	−0.01	0.04	
CE5C0400-YJFM00405	Lunar soil of CE-5	−0.04	0.04	0.01	0.04	3
		−0.03	0.06	0.01	0.04	3
		−0.06	0.03	0.00	0.02	3
Average		−0.04	0.04	0.01	0.04	
CE5C0400-YJFM00406	Lunar soil of CE-5	0.00	0.05	0.02	0.08	3
		0.01	0.01	−0.01	0.03	3
		−0.04	0.06	−0.04	0.06	3
Average		−0.01	0.04	−0.01	0.06	
CE5C0600	Lunar soil of CE-5	−0.16	0.04	−0.06	0.03	3
		−0.12	0.03	−0.05	0.06	6
Average		−0.13	0.03	−0.05	0.05	
CE5C0800YJYX038	Lunar rock clast of CE-5	−0.33	0.05	−0.17	0.06	6
CE6C0400YJFM004-R003	Lunar soil of CE-6	0.04	0.05	0.05	0.05	6
CE6C0400YJFM004-C047	Lunar clasts in CE-6 soil	−0.17	0.01	−0.07	0.06	6
NWA11273	Feldspathic breccia	−0.25	0.01	−0.13	0.07	3
DAG400	Anorthositic breccia	−0.21	0.05	−0.09	0.03	3
NWA5744	Granulitic troctolitic breccia	−0.27	0.02	−0.14	0.02	3
NWA10756	Feldspathic breccia	−0.29	0.04	−0.12	0.01	3
NWA12971	Troctolitic melt rock	−0.19	0.04	−0.11	0.03	9
NWA13582	Feldspathic breccia	−0.20	0.03	−0.04	0.04	12
BHVO-2	Basalt	−0.29	0.02	−0.14	0.03	3
		−0.29	0.02	−0.16	0.02	6
		−0.29	0.03	−0.14	0.02	6
AGV-2	Andesite	−0.20	0.05	−0.11	0.03	3

Silicon isotope signatures of the source materials of the CE-5 and CE-6 lunar soils

The CE-5 basalt clast analyzed in this study is a fragment from a lava flow. Its Mg and Fe isotopic compositions have been measured by a previous study, and the results indicate that the mantle source of the lava contains cumulates of both early and late stages of the lunar magma ocean[19]. This clast was not affected by evaporation during later impacts[19], meaning that its Si isotope compositions primarily reflect the composition of basalt. The higher δ^{30}Si of the CE-5 lunar soils compared to the basalt clast suggests that their original Si isotopic signatures were modified by subsequent processes. Physical property studies suggest that 95% of the particle sizes of CE-5 soils range from 4.84 μm to 432.27 μm (mean 49.80 μm by mass) and from 1.40 μm to 9.35 μm (mean 3.96 μm by number)[20,21]. The particle size distribution is similar to that of Apollo lunar soils[22], indicating an intense weathering process. CE-5 soils are the fine mixture of local basalt with a small portion of exotic materials, including <5 wt% of ejected highland material and Rare Earth Element- and phosphorous-rich (KREEP) basalts (from other locations on the moon), as well as ~1 wt% of meteoritic material[23]. Based on the Si isotope data of Apollo samples[13–16], the highland materials and KREEP basalts likely have Si isotopes similar to or slightly heavier than BSE[18]. The SiO_2 content of Apollo lunar rocks, including high- and low-Ti basalts, highland suites,

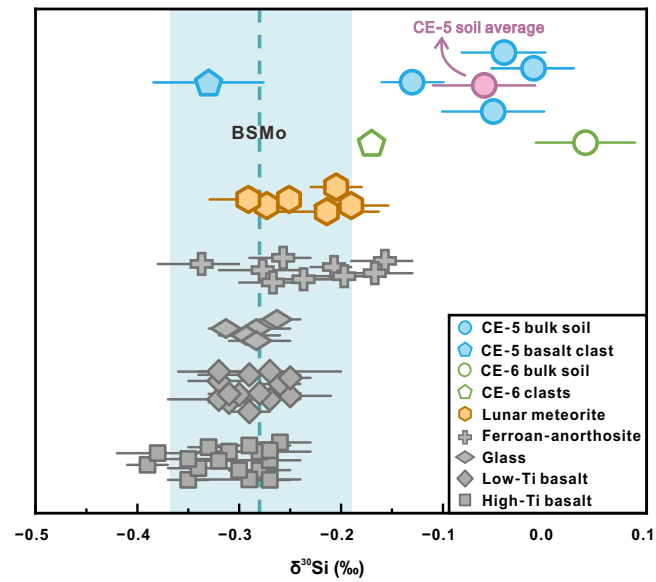

Fig. 1 | Silicon isotopic data of Chang'E samples and lunar meteorites in this study, compared with Apollo samples from the literature (gray symbols). Data for Apollo samples and the BSMo average value are from refs. 13–17, with error bars representing two standard deviations or two standard errors. All lunar soils exhibit heavier Si isotopic compositions than BSMo (light green range). The δ^{30}Si value of CE-6 bulk soil (green hollow circle) is higher than that of CE-5 soils (blue solid circle). In contrast, the δ^{30}Si values of CE-5 clasts (blue solid pentagon), and lunar meteorites (yellow solid hexagon) fall within the BSMo range, similar to Apollo sample (gray symbols) from the literature. The δ^{30}Si value of CE-6 clast is slightly heavier than that of CE-5 clast.

https://doi.org/10.1038/s41467-025-59577-6

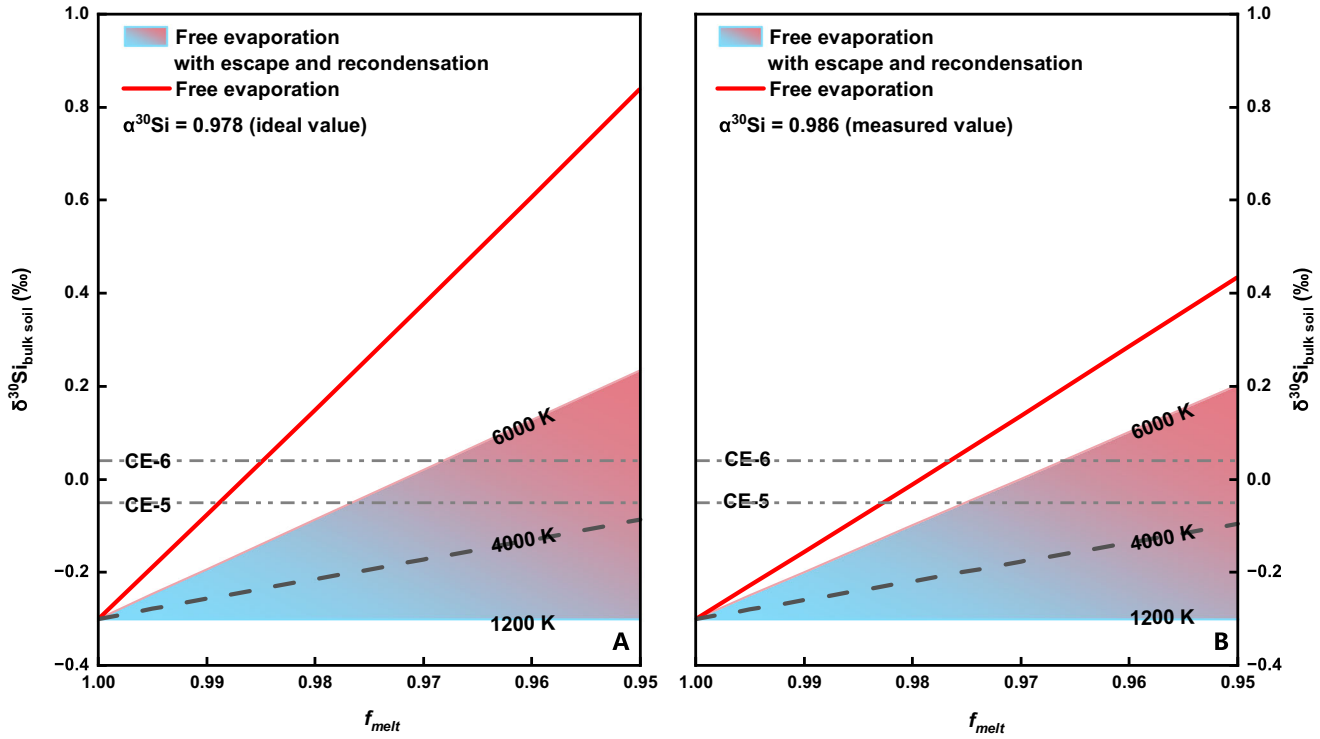

Fig. 2 | The calculated $\delta^{30}Si_{soil}$ values of the residue soil after evaporation. The effect of escape under different temperatures has been included in the calculation. Two different $\alpha_{^{30}Si}$ values are used in the calculation. (A) The ideal value of $\alpha_{^{30}SiO}$ is calculated by $\alpha_{^{30}SiO} = \sqrt{\frac{m^{28}SiO}{m^{30}SiO}}$, while (B) the measured $\alpha_{^{30}SiO}$ value of 0.98577 from experiment based on partial evaporation from Type B CAI liquids into vacuum[44]. f_{melt} represents the fraction of the residue soil in the evaporation process. The red line represents the free evaporation process, while the colored area represents the combined effects of free evaporation, partial escape, and full recondensation processes. The sloped gray dotted line indicates a temperature scenario of 4000 K, and the horizontal gray dotted lines denote the mean $\delta^{30}Si$ values of CE-5 and CE-6 soils.

and KREEP basalts, ranges from approximately 36 wt% to ~57 wt%[15]. The SiO_2 content of the CE-5 lunar soils, at around 38 wt% to 43 wt%, falls within this range. Thus, the addition of 5% exotic materials from highland and KREEP basalts would not significantly change the Si isotopic composition of the lunar soils.

Most meteorites, except for angrites, have lower $\delta^{30}Si$ compared to lunar samples (e.g., see ref. 24). Therefore, the addition of meteoritic material to lunar soils might slightly, but not significantly, change their Si isotopic composition (Supplementary Fig. 1). For instance, adding 1% (by mass) of meteorites with the lightest Si isotopic composition ever reported (−0.77‰, see ref. 25) and SiO_2 content of 45.0 wt% (the highest of SiO_2 content reported by Armytage et al.[26]) could decrease the total $\delta^{30}Si$ value of the lunar soil by only 0.01‰ (Supplementary Fig. 1, Supplementary Table 2), a change too small to detect within error. As a result, the original Si isotopic composition of the CE-5 lunar soils should primarily reflect that of the local basalt, but has been subsequently modified by space weathering processes.

In terms of maturity, the CE-6 and CE-5 samples are similar. Most (95%) of the particle sizes of CE-6 range from 5.97 μm to 382.36 μm (mean 85.86 μm by mass) and from 1.11 μm to 10.77 μm (mean 5.41 μm by number)[12]. In contrast to the CE-5 soils, the CE-6 lunar soil contains at least 13% foreign material, primarily non-basaltic ejecta, which may originate from the lunar highland crust, South Pole-Aitken (SPA) impact melts, and potentially early lunar mantle[12]. If meteoritic material was a major component of the non-basaltic ejecta, it would have reduced the $\delta^{30}Si$ of the CE-6 soil (Supplementary Fig. 1), which was not observed in this study. Therefore, most of the foreign material in the CE-6 lunar soil is unlikely to be meteorites. Compared to the CE-5 soil, the CE-6 soil has a lower density (3.035 g/cm^3 vs. 3.195 g/cm^3) and contains less olivine but more light-colored particles, such as plagioclase and amorphous glass[12]. The $\delta^{30}Si$ of the combined CE-6 clasts (−0.17 ± 0.01‰, 2 SD) falls in the range observed in ferroan-anorthosite from the Apollo missions[13,15], which likely reflects the addition of plagioclase, as plagioclase tends to have heavier Si isotopes than clinopyroxene (cpx)[27,28]. The primary plagioclase in the CE-6 soil is anorthite (82.96%, see ref. 12). According to first-principles calculation results, when crystallization temperature varies from 1600 K to 2000 K, the Si isotope fractionation between anorthite and cpx ranges from 0.13‰ to 0.07‰[27,28]. If all 13% foreign material added to the CE-6 soil was anorthite fragment or ejecta derived from anorthite[12], the $\delta^{30}Si$ should be increased by 0.01‰ to 0.02‰, a minor change insufficient to account for the high $\delta^{30}Si$ observed in the CE-6 soil. Meanwhile, the bulk composition of the CE-6 clasts shows that anorthosite material is not the main constituent, with Al_2O_3 (16.6 wt%), CaO (10.3 wt%), and SiO_2 (53.1 wt%). Therefore, though the addition of anorthite may slightly increase the $\delta^{30}Si$, it is not the primary cause of the heavy Si isotope compositions in the CE-6 soil. The elevated $\delta^{30}Si$ in the bulk CE-6 soil is more likely a result of modification by space weathering.

The Si isotopic signatures of lunar soils recorded the effects of space weathering

Space weathering, including micrometeorite impact and solar wind irradiation with ion sputtering, can melt minerals to cause evaporation, changing the isotopic composition of lunar soils (e.g., see refs. 2,7). Previous studies observed that both micrometeorite impact vaporization and ion sputtering modified K and Rb isotopes in Apollo mission soils. Elements with lower surface binding energy are more susceptible to ion sputtering, causing larger isotope fractionation. The surface binding energy of Si is 4.72 eV, which is significantly higher than Ca (1.84 eV) and Mg (1.51 eV), and slightly higher than Fe (4.28 eV)[29]. So, if ion sputtering was the dominant process during space weathering to affect Ca, Mg, and Si isotopes, the fractionation of

Si isotopes should be much less pronounced compared to that of Ca and Mg in the Chang'E lunar soils. However, the observed Si isotope fractionation ($\Delta^{30}Si_{soil\text{-}clast} = \delta^{30}Si_{lunar\ soil} - \delta^{30}Si_{basaltic\ clast}$) between CE-5 lunar soil and basaltic clast is 0.32‰ and between CE-6 bulk soil and clasts is 0.21‰, both of which are larger than the Mg and Fe isotope fractionation ($\Delta^{26}Mg_{soil\text{-}clast} = 0.100‰$ and $\Delta^{56}Fe_{soil\text{-}clast} = 0.173‰$) between CE-5 lunar soil and basaltic clast[3,19], while the $\delta^{26}Mg_{lunar\ soil}$ and $\delta^{56}Fe_{lunar\ soil}$ of CE-6 samples have not been reported yet. Therefore, solar wind sputtering is unlikely to be the dominant mechanism for Si isotope fractionation. Instead, evaporation by micrometeorite impact may be the primary process.

Micrometeorite impacts can produce shock-induced melts, forming silicon oxide nanoparticles ($npSiO_x$) and nanophase iron (npFe) in Apollo 15 soil pyroxene grains[30]. Similarly, in CE-5 soil olivine grains, vesicles containing oxygen-rich (npSiO and O_2) components were observed in weathered rims[10]. This suggests that micrometeorite impacts commonly cause surface grain melting and SiO (or $npSiO_x$) evaporation. Previous studies observed that the surface of CE-5 olivine grains exhibits unique vesicular $npFe^0$ and Si-rich materials, which formed by olivine decomposition at subsolidus temperature (~930 °C or 1200 K). This suggests that CE-5 samples experienced a lower temperature induced by micro-impact compared with Apollo soil samples[2,10]. The Fe and Mg isotopic variation of CE-5 lunar soils and the major element ratios of MgO/Al_2O_3 or FeO/Al_2O_3 support that free evaporation is a primary process responsible for isotopic fractionation in lunar soils[3]. During free evaporation, SiO vapor becomes enriched in lighter Si isotopes, while the remaining melt is enriched in heavier isotopes (Fig. 2, details see Computational methods)[8,9]. With more evaporation loss of SiO during free evaporation, the $\delta^{30}Si_{bulk\ soil}$ would increase, reaching the values measured in CE-5 soil in this study. Micrometeorite impact can also enrich heavy K and Rb isotopes in lunar soils, but free evaporation models show that the impact alone cannot produce the high $\delta^{41}K$ and $\delta^{87}Rb$ values in Apollo soils observed in ref. 2.(Supplementary Fig. 2, Supplementary Table 3). This is consistent with the conclusion of ref. 2 that the ion sputtering can also contribute to the heavier K and Rb isotope compositions in Apollo lunar soils. Therefore, multiple isotope variations can be used to constrain the influence of different processes on the lunar surface.

The partial melting temperatures induced by micro-impact in CE-6 lunar soils have not yet been evaluated, so the estimated temperatures are used in this study. If CE-6 samples experienced conditions similar to CE-5 soils, the effect of free evaporation on Si isotopes will be similar. If CE-6 samples experienced conditions similar to Apollo samples, the vapor temperature could range from 2500 K to 5000 K, depending on impact velocity[31,32]. The micrometeorite with a higher impact velocity and larger mass would produce a higher melting temperature. At these higher temperatures that of CE-6 sample may have experienced, greater evaporation could be produced. During free evaporation, with f_{melt} (the fraction of Si remaining in the residual melt) decreasing, the $\delta^{30}Si$ of bulk soil is increasing (Fig. 2).

With melting temperature increasing, vapor has sufficient energy to exceed lunar escape velocity and leave the lunar atmosphere into the space[33]. The lost fractions and isotopic fractionations of escape can be calculated based on the energy (temperature) of the released atoms (see Computational methods and Supplementary Information for the details). Although light isotopes preferentially escape, leaving the remaining vapor relatively enriched in heavy isotopes, the remaining vapor still inherited the light Si isotope characteristics of the original vapor.

Vapor-deposited layers have been observed on minerals exposed on the surface of CE-5 soil[11], Apollo soil grains (e.g., see refs. 34,35) and on dust grains from the Itokawa asteroid (e.g., see refs. 36,37), indicating that condensation processes are widespread in lunar soils. If residual SiO vapor deposits onto soil grain surfaces, it is still enriched in light Si isotopes relative to the initial soil, and could decrease $\delta^{30}Si$ of lunar soil after evaporation (Fig. 2). Because the loss of light Si isotopes into the space (Supplementary Table 4 and Supplementary Table 5), the bulk Si isotope composition combining Si in both the residual soil and condensed material should still be heavier than the initial value before space weathering (Fig. 2 and Supplementary Table 5). Therefore, if the deposit layer on CE-5 and CE-6 soil is from the residual vapor with escape losses, it could still exhibit higher $\delta^{30}Si$ than the initial soil (Fig. 2). The space weathering process experienced by Chang'E samples is simplified into a conceptual diagram (Fig. 3).

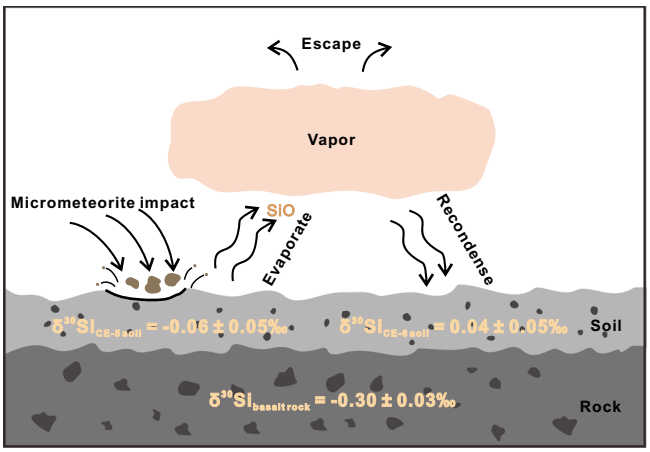

Fig. 3 | The conceptual diagram illustrates the simplified space weathering process experienced by Chang'E samples. The mean $\delta^{30}Si$ value of lunar basalts is derived from Apollo data[13–16] and CE-5 lunar clast data obtained in this study. The mean $\delta^{30}Si$ value of CE-5 and CE-6 soils is from this study. The light pink shaded region represents the vapor generated by free evaporation.

The Si isotope difference between CE-5 and CE-6 lunar soils

The $\delta^{30}Si$ value of the CE-6 bulk soil is higher than the average $\delta^{30}Si$ of the CE-5 soil, and the clasts from the CE-6 soil also show a higher $\delta^{30}Si$ value than the basalt clast from CE-5 (Fig. 1). Since the CE-6 clasts (~200 μm each) are much smaller than the basalt clast of CE-5 (>1 mm), space weathering may have a more pronounced effect on the Si isotopes of these smaller ones, while the bigger clast is more resistant to weathering. Isotope analyses of sieved soils indicate that grains larger than 180 μm have heavier Fe and Mg isotopic compositions than the basalt clast, but lighter than the bulk soil[3]. That suggests that grains larger than 180 μm in the CE-5 soil are also affected by space weathering. Thus, it is likely that the Si isotopic composition of the CE-6 clasts also reflects the influence of space weathering.

Since the added anorthite cannot significantly enhance the $\delta^{30}Si$ value of lunar soil, the heavier Si isotopic composition in the CE-6 bulk soil than the CE-5 bulk soil is primarily attributed to space weathering. It is possible that the temperature induced by micro-impacts in CE-6 lunar soils is similar to that in Apollo samples, but higher than that in CE-5 soils, which might result in a higher degree of evaporation and a larger Si isotope fractionation. Due to the higher temperature, the free evaporation degree of CE-6 soil is higher than that of CE-5 soil, which can produce heavier Si isotopes in the soil. Also, the vapor produced by evaporation during CE-6 soil melting has higher energy than that from CE-5 soils, leading to greater mass loss and more pronounced isotopic effects through vapor escape. These could explain the heavier Si isotopic composition in CE-6 soil relative to CE-5 soils.

Although it is not exactly clear how the space weathering fractionates Si isotopes, there are two possible explanations for the Si isotopic offset between the CE-5 and CE-6 samples:

1. Duration of Space Weathering: the CE-6 lunar soil may have a longer exposure time than the CE-5 soil which makes it undergo a longer period of weathering with a greater frequency of micrometeorite impacts and results in heavier Si isotopic compositions.

2. Location on the farside of the moon: the CE-6 lunar soil was collected from the farside of the Moon, which may have undergone processes different from those on the nearside. For instance, due to the influence of Earth's gravity, the nearside may experience fewer micrometeorite impacts than the farside. More frequent impacts on the farside could lead to more intensive evaporation, potentially resulting in heavier Si isotopes.

Because the currently available Si isotope data alone are insufficient to determine the contribution of different weathering period and the influence of Earth's gravity on the difference in Si isotopes between CE-5 and CE-6 lunar soils, more petrographic evidence and isotope data of CE-6 samples, including soil and larger size of clasts, are needed to clarify the key mechanisms of space weathering.

Methods

Sample background

All CE-5 and CE-6 samples analyzed in this study were allocated by the China National Space Administration and are scooped samples. CE-5 mission landed in the Procellarum-KREEP Terrane (PKT) of the Moon (43.06°N, 51.92°W), representing the youngest mare basalt ever discovered (~2.0 Ga; see refs. 21,38,39). The CE-5 samples primarily consist of regolith, collected from a few centimeters below the surface and drilled from an approximately 1-meter-long core of lunar regolith[22].

The CE-6 mission landed at the edge of the SPA basin (41.625°S, 153.978°W), while the CE-6 samples were scooped from the southern edge of the Apollo crater, the largest crater within the SPA basin. CE-6 is the first returned sample from the Moon's farside[12]. The SPA basin is the largest, deepest, and oldest impact basin on the Moon, significantly differing from the lunar nearside in terms of crustal thickness, magma activity, and composition. Based on the statistical dating of impact craters, the basalt strata near the CE-6 landing site are estimated to be ~2.79~2.87 Ga[12]. Unlike the CE-5 soil, the CE-6 soil exhibits a mixture of various compositions, including at least ~13% exotic materials in addition to basaltic material[12].

Sample purification and isotope analysis

Silicon purification and isotope analysis were performed at the State Key Laboratory of Lithospheric and Environmental Coevolution, University of Science and Technology of China (USTC), Hefei. The method used to determine the Si isotopic composition was modified from published work[40]. Approximately 0.6–2.3 mg of powdered CE-5, CE-6 samples and meteorites were weighted into silver crucibles and subsequently fused with ~100 mg high-purity NaOH at 720 °C for 10 min in a furnace. After cooling to room temperature, the fusion cake was dissolved in 15 mL of ultrapure water (18.2 MΩ cm, Millipore) in a Teflon container and left under room temperature overnight. A small amount (~0.2 mL) of concentrated HNO_3 (15.4 mol/L) was then added to adjust the pH of the solution to between 1 and 2. The final Si concentration is typically between 15 and 20 μg/g.

Silicon was purified using ion-chromatography with 2 mL Bio-Rad AG50 W-X12 cation resin (200–400 mesh) in a 10 mL Bio-Rad polypropylene column[40]. Prior to loading samples, the resin was precleaned with ultrapure water and 6 mol/L HNO_3. After the resin was conditioned with 6 mL ultrapure water, 4 mL sample solution was loaded. Silicon was eluted immediately, following by an additional 5 mL ultrapure water to ensure complete elution. Reference materials NBS28 (quartz from the National Institute of Standards and Technology, NIST) and BHVO-2 (basalt from the United States Geological Survey, USGS) were processed using the same digestion and purification procedures. The total procedural blank was 44 ng, negligible compared to the Si loading (~60–80 μg).

Silicon isotopes were analyzed using multicollector inductively coupled plasma–mass spectrometry (MC–ICP–MS, Neptune Plus) from Thermo–Fisher Scientific (Bremen, Germany) at the same laboratory at USTC. Sample solutions were introduced into the instrument through a PFA microflow nebulizer (ESI) with an ~50 μL/min aspiration rate, a quartz dual cyclonic spray chamber, and nickel H skimmer and jet cones. During analysis, the ^{28}Si, ^{29}Si, and ^{30}Si were collected in L3, C, and H3 Faraday cups, respectively, under high-resolution mode. The details of the instrumental parameters are listed in Supplementary Table 6. The signal sensitivity for ^{28}Si is ~4 V/(μg/g), and the sample solution concentration used for isotope analysis was ~3 μg/g. Instrumental mass bias was corrected using the standard-sample bracketing (SSB) method, with NBS28 as the standard. Silicon isotopes are expressed in delta notation as $\delta^{30}Si$ (‰) = $[(^{30}Si/^{28}Si)_{sample}/(^{30}Si/^{28}Si)_{NBS28} - 1] \times 1000$. On the three-isotope diagram of Si (Supplementary Fig. 3), all samples and reference materials plot on a mass-dependent isotope fractionation line. The long-term precision for $\delta^{30}Si$ measurement of BHVO-2 was better than 0.06‰ (2 SD) for $\delta^{30}Si$[41]. The average $\delta^{30}Si$ value of BHVO-2 analyzed in this study was −0.29 ± 0.03‰ (n = 15, 2 SD), and that of AGV-2 was −0.20 ± 0.05‰ (n = 3, 2 SD), which are consistent with previously published values (e.g., see refs. 18,42,43). The $\delta^{30}Si$ of two rock standards agree with published values, and the results of replicates are consistent within error (Table 1), demonstrating the reliability of our data.

Computational methods

Both the evaporation of SiO gas from melt and the escape of SiO vapor into space can influence Si isotopes in lunar soils. During free evaporation, the evaporated material remains continuously isolated from exchange with the residue. Consequently, the fraction of the element remaining in the residue follows a Rayleigh fractionation equation:

$$R/R_0 = f_X^{\alpha_X - 1} \quad (1)$$

where $R = ({}^iX/{}^jX)_{residue}$, $R_O = ({}^iX/{}^jX)_{pre\text{-}evaporation}$, ${}^iX$ and ${}^jX$ are the isotopes i and j of element X, f_X denotes the fraction of element X remaining in the residue, and α_X is the kinetic isotope fractionation factor for isotopes of element X. In this study, two α_X values are selected in the calculation (Fig. 2). The first α_{SiO} (0.978) is the calculated value ($\alpha_{SiO} = \sqrt{\frac{m^{28}SiO}{m^{30}SiO}}$, where m is the molecular weight of the relevant species), while the second α_{SiO} (0.986) is the experiment measured value from partial evaporation from Type B CAI liquids into vacuum[44], which is slightly higher than the calculated one. The Si isotope ratio in residual melt is estimated using Rayleigh equation:

$$\Delta^{30}Si_{evaporation} = (\alpha - 1) \times 1000 \ln f_{melt} \quad (2)$$

where $\Delta^{30}Si_{evaporation}$ represents the difference of δ-notations between residual melt and initial pre-evaporation material, the f_{melt} is fraction of Si remaining in the residual melt. Regardless of which α_{SiO} value is used, similar results are obtained, indicating that the Si isotopes in the residue are enriched in heavier isotopes (Fig. 2). At temperatures between 1200 and 2000 K (the environment of CE-5 samples), most SiO gas remains in the lunar atmosphere or deposits on the surface without escaping (Supplementary Table 4). Therefore, free evaporation is the dominant process responsible for Si isotopic fractionation in CE-5 soils that experienced low-temperature impact events.

The fraction of vapor that escapes from the lunar surface can be estimated by assuming that vapor with kinetic energies exceeding the gravitational energy is lost to space[45]. According to the Boltzmann distribution, the fraction of particles with kinetic energies less than the gravitational binding energies is:

$$f_{bind} = 1 - \exp(-\lambda) \quad (3)$$

where λ is the Jeans escape parameter: $\lambda = GMm/(k_BTR)$, which G is the gravity parameter, M is the mass of planet, m is the mass of molecular,

k_B is the Boltzmann constant, T is the temperature (K), R is the radius of planet. The isotope ratio is estimated by the following equation:

$$\Delta^{30}Si_{escape} = 1000 \ln \frac{1 - \exp(-\lambda^{30}SiO)}{1 - \exp(-\lambda^{28}SiO)} \quad (4)$$

where $\Delta^{30}Si_{escape}$ is the difference in δ-notations between the residual vapor and the initial pre-escape vapor (Supplementary Table 5). The residual vapor after escape is enriched in heavier Si isotopes compared to the initial vapor. For CE-6 soils, which likely experienced high-temperature impact events, both evaporation and escape processes influence their Si isotopes. The overall fractionation effects are combined using mass-balance equations: $\delta^{30}Si_{bulk\ soil} = [f_{melt} \times (\delta^{30}Si_{basalt} + \Delta^{30}Si_{residue\ soil-basalt}) + f_{bind}\ (1 - f_{melt})\ (\delta^{30}Si_{basalt} - \frac{f_{melt}}{1-f_{melt}}\Delta^{30}Si_{residue\ soil-basalt} + \Delta^{30}Si_{residue-initial\ vapor})]/[f_{melt} + f_{bind}\ (1-f_{melt})]$.

Data availability

All data needed to evaluate the conclusions in the paper are present in the paper and/or the Supplementary Information.

References

1. McKay, D. S. et al. The lunar regolith. *Lunar Sourceb.* **567**, 285–356 (1991).
2. Nie, N. X., Dauphas, N., Zhang, Z. J., Hopp, T. & Sarantos, M. Lunar soil record of atmosphere loss over eons. *Sci. Adv.* **10**, eadm7074 (2024).
3. Shi, Q. et al. Elemental differentiation and isotopic fractionation during space weathering of Chang'E-5 lunar soil. *Geochim. Cosmochim. Acta* **378**, 127–143 (2024).
4. Moynier, F., Albarède, F. & Herzog, G. F. Isotopic composition of zinc, copper, and iron in lunar samples. *Geochim. Cosmochim. Acta* **70**, 6103–6117 (2006).
5. Sands, D., Rosman, K. & De Laeter, J. A preliminary study of cadmium mass fractionation in lunar soils. *Earth Planet Sci. Lett.* **186**, 103–111 (2001).
6. Wang, K., Moynier, F., Podosek, F. A. & Foriel, J. An iron isotope perspective on the origin of the nanophase metallic iron in lunar regolith. *Earth Planet Sci. Lett.* **337-338**, 17–24 (2012).
7. Wiesli, R. A., Beard, B. L., Taylor, L. A. & Johnson, C. M. Space weathering processes on airless bodies: Fe isotope fractionation in the lunar regolith. *Earth Planet Sci. Lett.* **216**, 457–465 (2003).
8. Clayton, R. N., Mayeda, T. K. & Epstein, S. Isotopic fractionation of silicon in Allende inclusions. In *Lunar and Planetary Science Conference*, 9th. 1267–1278 (Pergamon Press Inc., New York, 1978).
9. Dauphas, N., Poitrasson, F., Burkhardt, C., Kobayashi, H. & Kurosawa, K. Planetary and meteoritic Mg/Si and δ30Si variations inherited from solar nebula chemistry. *Earth Planet Sci. Lett.* **427**, 236–248 (2015).
10. Guo, Z. et al. Nanophase iron particles derived from fayalitic olivine decomposition in Chang'E-5 lunar soil: implications for thermal effects during impacts. *Geophys. Res. Lett.* **49**, e2021GL097323 (2022).
11. Gu, L. X. et al. Space weathering of the Chang'e-5 Lunar sample from a mid-high latitude region on the moon. *Geophys. Res. Lett.* **49**, e2022GL097875 (2022).
12. Li, C. et al. Nature of the lunar farside samples returned by the Chang'E-6 mission. *Natl Sci. Rev.* **11**, nwae328 (2024).
13. Poitrasson, F. & Zambardi, T. An Earth–Moon silicon isotope model to track silicic magma origins. *Geochim. Cosmochim. Acta* **167**, 301–312 (2015).
14. Georg, R. B., Halliday, A. N., Schauble, E. A. & Reynolds, B. C. Silicon in the Earth's core. *Nature* **447**, 1102–1106 (2007).
15. Armytage, R. M. G., Georg, R. B., Williams, H. M. & Halliday, A. N. Silicon isotopes in lunar rocks: implications for the Moon's formation and the early history of the Earth. *Geochim. Cosmochim. Acta* **77**, 504–514 (2012).
16. Fitoussi, C. & Bourdon, B. Silicon isotope evidence against an enstatite chondrite earth. *Science* **335**, 1477–1480 (2012).
17. Zambardi, T. et al. Silicon isotope variations in the inner solar system: implications for planetary formation, differentiation and composition. *Geochim. Cosmochim. Acta* **121**, 67–83 (2013).
18. Savage, P. S., Georg, R. B., Armytage, R. M. G., Williams, H. M. & Halliday, A. N. Silicon isotope homogeneity in the mantle. *Earth Planet Sci. Lett.* **295**, 139–146 (2010).
19. Jiang, Y. et al. Fe and Mg isotope compositions indicate a hybrid mantle source for young Chang'E 5 mare basalts. *ApJL* **945**, L26 (2023).
20. Cao, K. et al. A novel method for simultaneous analysis of particle size and mineralogy for Chang'E-5 lunar soil with minimum sample consumption. *Sci. China Earth Sci.* **65**, 1704–1714 (2022).
21. Li, C. et al. Characteristics of the lunar samples returned by the Chang'E-5 mission. *Natl. Sci. Rev.* **9**, nwab188 (2022).
22. Chen, Y. et al. Chang'e-5 lunar samples shed new light on the moon. *Innov. Geosci.* **1**, 100014 (2023).
23. Zong, K. et al. Bulk compositions of the Chang'E-5 lunar soil: Insights into chemical homogeneity, exotic addition, and origin of landing site basalts. *Geochim. Cosmochim. Acta* **335**, 284–296 (2022).
24. Poitrasson, F. Silicon isotope geochemistry. *Rev. Miner. Geochem.* **82**, 289–344 (2017).
25. Savage, P. S. & Moynier, F. Silicon isotopic variation in enstatite meteorites: clues to their origin and earth-forming material. *Earth Planet Sci. Lett.* **361**, 487–496 (2013).
26. Armytage, R. M. G., Georg, R. B., Savage, P. S., Williams, H. M. & Halliday, A. N. Silicon isotopes in meteorites and planetary core formation. *Geochim. Cosmochim. Acta* **75**, 3662–3676 (2011).
27. Huang, F., Wu, Z., Huang, S. & Wu, F. First-principles calculations of equilibrium silicon isotope fractionation among mantle minerals. *Geochim. Cosmochim. Acta* **140**, 509–520 (2014).
28. Qin, T., Wu, F., Wu, Z. & Huang, F. First-principles calculations of equilibrium fractionation of O and Si isotopes in quartz, albite, anorthite, and zircon. *Contrib. Miner. Pet.* **171**, 1–14 (2016).
29. Schaible, M. J. et al. Solar wind sputtering rates of small bodies and ion mass spectrometry detection of secondary ions. *J. Geophys. Res. Planets* **122**, 1968–1983 (2017).
30. Gu, L. et al. The discovery of silicon oxide nanoparticles in space-weathered of Apollo 15 lunar soil grains. *Icarus* **303**, 47–52 (2018).
31. Eichhorn, G. 2.2. 8 Impact light flash studies: temperature, ejecta, vaporization. In *International Astronomical Union Colloquium* (Cambridge University Press, 1976).
32. Eichhorn, G. Heating and vaporization during hypervelocity particle impact. *Planet Space Sci.* **26**, 463–467 (1978).
33. Wurz, P. et al. Particles and photons as drivers for particle release from the surfaces of the Moon and Mercury. *Space Sci. Rev.* **218**, 10 (2022).
34. Keller, L. P. & McKay, D. S. Discovery of vapor deposits in the lunar regolith. *Science* **261**, 1305–1307 (1993).
35. Keller, L. P. & McKay, D. S. The nature and origin of rims on lunar soil grains. *Geochim. Cosmochim. Acta* **61**, 2331–2341 (1997).
36. Noguchi, T. et al. Space weathered rims found on the surfaces of the Itokawa dust particles. *Meteorit. Planet Sci.* **49**, 188–214 (2014).
37. Thompson, M. S., Christoffersen, R., Zega, T. J. & Keller, L. P. Microchemical and structural evidence for space weathering in soils from asteroid Itokawa. *Earth Planets Space* **66**, 1–10 (2014).
38. Che, X. et al. Age and composition of young basalts on the Moon, measured from samples returned by Chang'e-5. *Science* **374**, 887–890 (2021).
39. Li, Q. L. et al. Two-billion-year-old volcanism on the Moon from Chang'e-5 basalts. *Nature* **600**, 54–58 (2021).

40. Georg, R. B., Reynolds, B. C., Frank, M. & Halliday, A. N. New sample preparation techniques for the determination of Si isotopic compositions using MC-ICPMS. *Chem. Geol.* **235**, 95–104 (2006).
41. Yu, H.-M., Yang, L., Zhang, G.-L. & Huang, F. Silicon isotopic compositions of altered oceanic crust samples from IODP U1365 and U1368: effect of low-temperature seawater alteration. *Chem. Geol.* **624**, 121424 (2023).
42. Yu, H.-M., Li, Y.-H., Gao, Y.-J., Huang, J. & Huang, F. Silicon isotopic compositions of altered oceanic crust: implications for Si isotope heterogeneity in the mantle. *Chem. Geol.* **479**, 1–9 (2018).
43. Zambardi, T. & Poitrasson, F. Precise determination of silicon isotopes in silicate rock reference materials by MC-ICP-MS. *Geostand. Geoanal. Res.* **35**, 89–99 (2011).
44. Knight, K. B. et al. Silicon isotopic fractionation of CAI-like vacuum evaporation residues. *Geochim. Cosmochim. Acta* **73**, 6390–6401 (2009).
45. Erkaev, N. V., Lammer, H., Odert, P., Kulikov, Y. N. & Kislyakova, K. G. Extreme hydrodynamic atmospheric loss near the critical thermal escape regime. *Mon. Not. R. Astron. Soc.* **448**, 1916–1921 (2015).

Acknowledgements

National Natural Science Foundation of China (grant no. 42241102 to L.Q. and H.Y., and 42173003 to H.Y.). Anhui Provincial Natural Science Foundation (grant no. 2308085J06 to H.Y.).

Author contributions

H.Y. and F.H. contributed conceptualization. H.Z., Y.L., L.Y., and H.Y. contributed methodology. F.H., L.Q., J.S., and J.K. contributed samples. H.Z., H.Y. contributed figures and tables. Z.X., H.Z., H.T., and H.Y. contributed to the model. H.Y., H.Z., and F.H. contributed to the writing of the original draft. H.Z., H.Y., L.Q., and F.H. contributed review and editing.

Competing interests

The authors declare no competing interests.

Additional information

Supplementary information The online version contains supplementary material available at https://doi.org/10.1038/s41467-025-59577-6.

Correspondence and requests for materials should be addressed to Hui-Min Yu, Liping Qin or Fang Huang.

Peer review information *Nature Communications* thanks Deborah Domingue and the other, anonymous, reviewer for their contribution to the peer review of this work. A peer review file is available.